

The numerical simulation of contact between rail-wheel using FEA

I Blanari¹, V Goanță¹ and M Alexandrov¹

¹Mechanical Engineering Department, “Gheorghe Asachi” Technical University of Iasi, Iasi, Romania

E-mail: blanariigor@gmail.com

Abstract. The most important areas of study in Railway Engineering are the mechanics of rail-wheel contact, requiring both vast application expertise, diagnosis and the dependable analysis approach. In some specialized sources, the model used is 2D – model axisymmetric or a 3D – model using the poor mesh quality and the FEA boundary conditions is used with some approximations. In this paper is presented the simulation of contact between wheel and rail, the scenarios used different contact conditions using the Finite Element Method with the realistic 3D – solution.

1. Introduction

Taking into account the trends of the traffic speeds, increase axle load, but also to reduce the loss of material from the wheel or the rail due to wear phenomena, the appearance of wavy wear, fracture of the wheel and the rail, it is necessary to know the pressure distribution and the stress state at the wheel - rail contact. This can be achieved by the finite element method (FEM). The calculation of these stresses becomes much more complex for 3 dimensional (3D) real life geometries. Therefore, in the analytical studies mostly two-special geometry cases commonly used due to their simplicity to analyse. These are sphere-on-sphere and cylinder-on-cylinder cases where the radii of curvature of the contacting surfaces, can be varied ($\text{radii} \rightarrow \infty$ for plane surfaces) to obtain sub-cases of sphere-on-plane, sphere-in-cup, cylinder-on-plane, and cylinder-in-trough. In the literature [1-3] for some of such cases, closed form of analytical equations to calculate, the components of contact or Hertzian stresses presented. These equations are derived for above cases utilizing only elastic material properties (elastic-plastic material properties are omitted) and generally do not account for friction coefficient between the wheel and rail. Further, when wheel-rail contact geometry is complicated, the closed form of stress equations derived for simple contact geometries become approximate or invalid.

Rail-wheel systems (with complex contact geometries) utilize friction to transform power; as a consequence in such a system wheel-rail damages occur by the rolling contact and slip/stick mechanisms during contact in the form of wear or crack initiation/growth in the rails. It is a railway engineer's objective to accurately formulate or analyse this problem. Therefore, an understanding of the contact mechanism (stresses and pressure magnitudes/distributions) is important to estimate the



crack behaviours. Further wheel – rail wear/damage best modelled when the out coming 3D stresses and their corresponding orientations are calculated properly [4, 5].

Analysis of rail–wheel contact studied by many researchers in different context with different rail/wheel geometries to calculate Hertzian contact behaviour and find out stress distributions at the area of interest. As a consequence damage mechanisms such as surface cracks, plastic deformation, wear and operating rolling noise are also investigated. Proper understanding/simulation of these mechanisms served for clear understanding of a detailed knowledge of physical interaction between wheel and rail. In the literature [6-10], some of these issues studied using some experimental observations, analytical calculations and FEA calculations within various contexts.

In this study, it is intended to show a well known FEA procedure on an example 3D rail–wheel and axle model therefore more insight on the literature review and fundamentals of the problem of interest left out of the scope of this paper. In this work, the following steps regarding the 3D contact analysis of rail–wheel taken into consideration as in the following order and depicted in Figure 1:

- Design of rail and wheel assembly.
- Elastic-plastic material model.
- Boundary and loading conditions.
- Contact conditions where is included the different coefficient of frictions.
- Solve and post-processing the results.

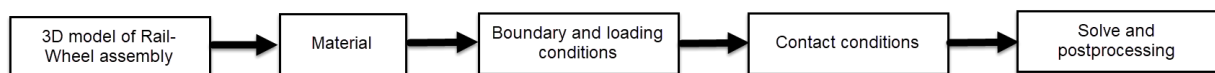


Figure 1. Simulation procedure.

2. FEA method

In this study, is used a mono-block wheel with 760 [mm] in diameter and profile S78 [11], the corresponding rail UIC 60 [12] and the axle, tilting the rail: 1/20, gauge: 1435 [mm], the distance between the inner faces of the two wheels: 1360 [mm], angle of attack: 0° and the friction is considered to be null in the longitudinal and transverse direction, the geometries are created in Autodesk Inventor 2017 and the assembly of the half of the symmetric model is presented in Figure 2.

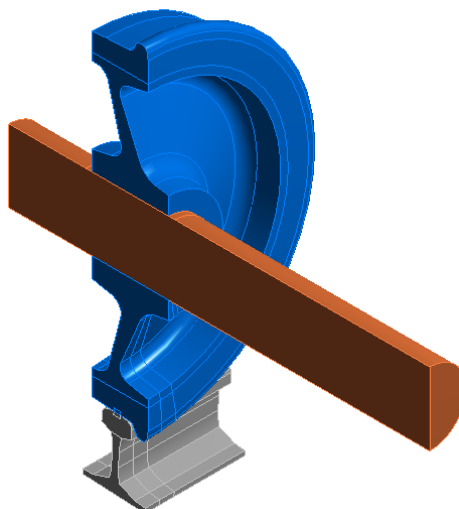


Figure 2. Geometry of the half of the symmetric model.

The material's model is adapted from the experimental data, where bi-linear elastic-plastic model is used and the material properties presented in Table 1 and Figure 3, respectively.

Table 1. The mechanical characteristics of material used in FEA scenarios.

Steel	ρ (density) [kg/m ³]	σ_a [MPa]	σ_r [MPa]	E [GPa]	ν
R7T (wheel)	7850	390	870	210	0,3
A2 (Axle)	7850	350	620	210	0,3
900A (rail)	7850	594	905	200	0,304

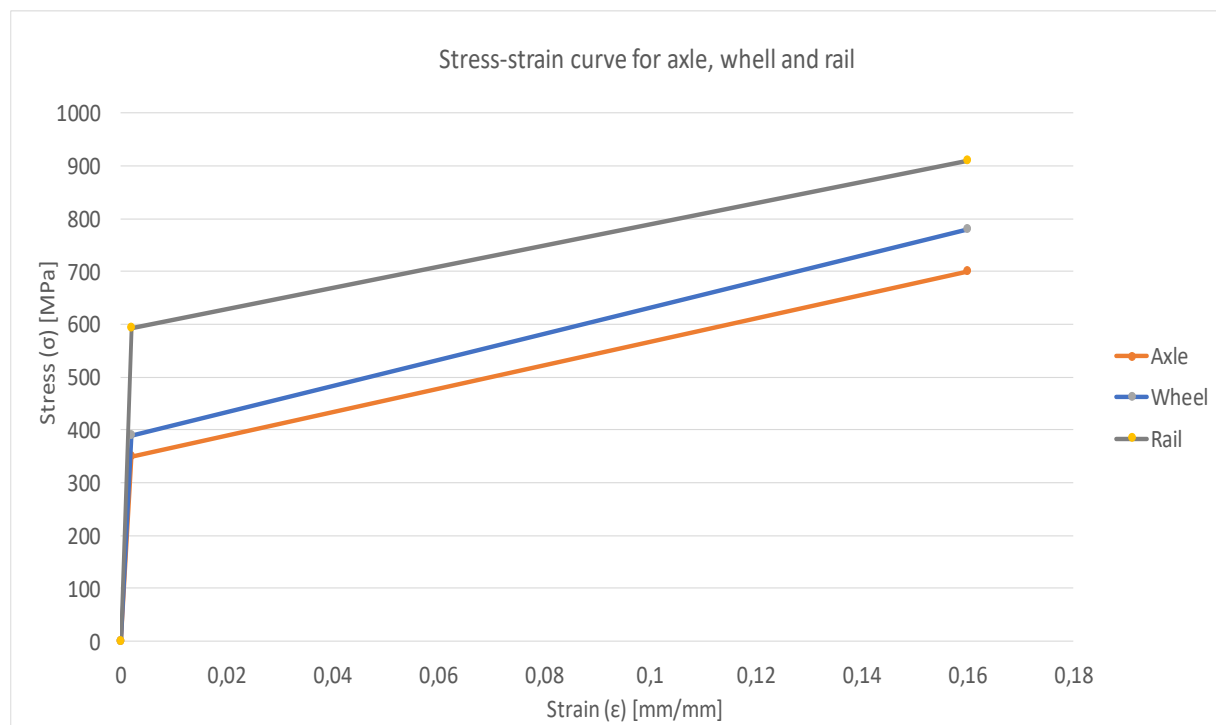


Figure 3. The models of the ensemble's materials.

The geometry model transferred in the CAE software and meshed solid185 8-node hex mesh elements as shown in Figure 4. The contact zone is mesh very well and shown to in Figure 4. The contact is modeled with the conta174 elements placed on wheel and target170 placed on rail. The FEA model mesh contained 190572 nodes and 204846 elements for all geometry. Loading conditions is presented in Figure 5, on half of wheel is applied a vertical force with a magnitude of 55 [kN]. Rail is fixed at traverse location at all direction for prevented body motion. The effects of rotational wheel and lateral force neglected. The FE model expected to represent more realistic way for load transfer between the axle – wheel – rail. And the thermal variation is also neglected. Friction coefficient presented in Table 2.

Table 2. Friction coefficient used in FEA scenarios.

μ	0	0,03	0,05	0,07	0,1	0,12	0,15	0,18	0,2	0,25
μ	0,3	0,35	0,4	0,45	0,5	0,55	0,6	0,65	0,7	

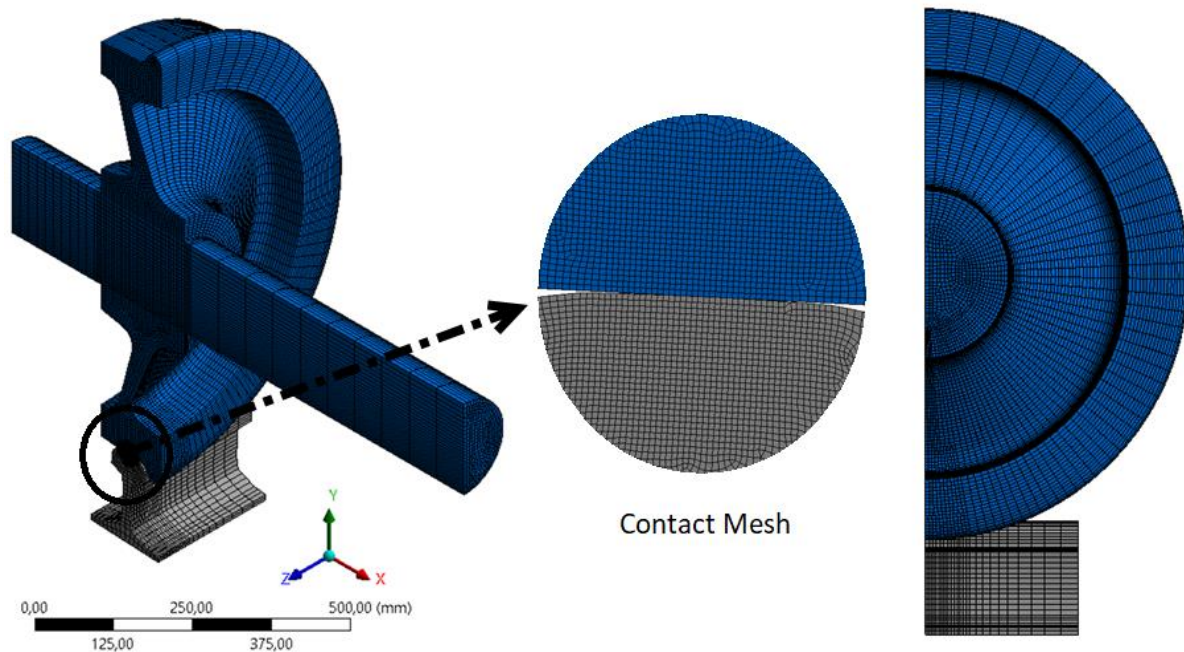


Figure 4. Mesh model.

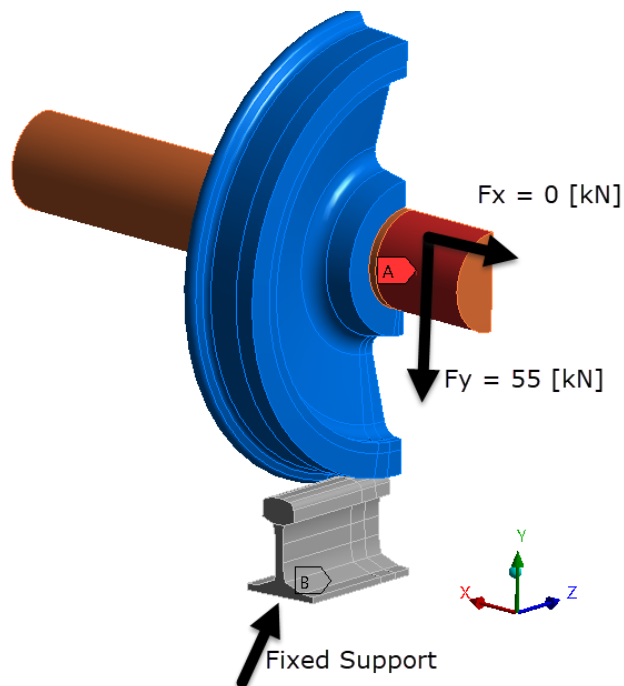


Figure 5. Boundary and loading conditions.

3. Post processing.

Final FE model is run and post-processed successfully to visualize stress and strain distributions. The maximum stress distribution is for coefficient of friction bigger than 0,1 presented in Figure 6.

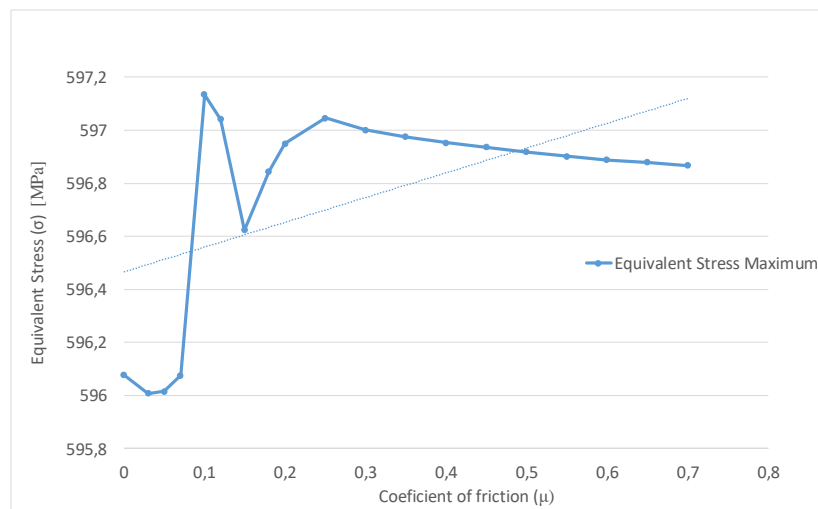


Figure 6. Maximum von Mises stress [MPa] versus coefficient of friction.

In Fig. 7-9, von Mises stress is plotted for both wheel and rail in the case of the coefficient of friction $\mu = 0,25$, as expected maximum stress is found 2.9851 mm inside of the outer surface around 597 MPa, above the yield limit for rail material. As the wheel maximum stress is found 3.2951 mm inside of the outer surface around 462,72 MPa, well above the yield limit for rail material, for both parts elastic-plastic deformations are observed for certain regions as shown in the following.

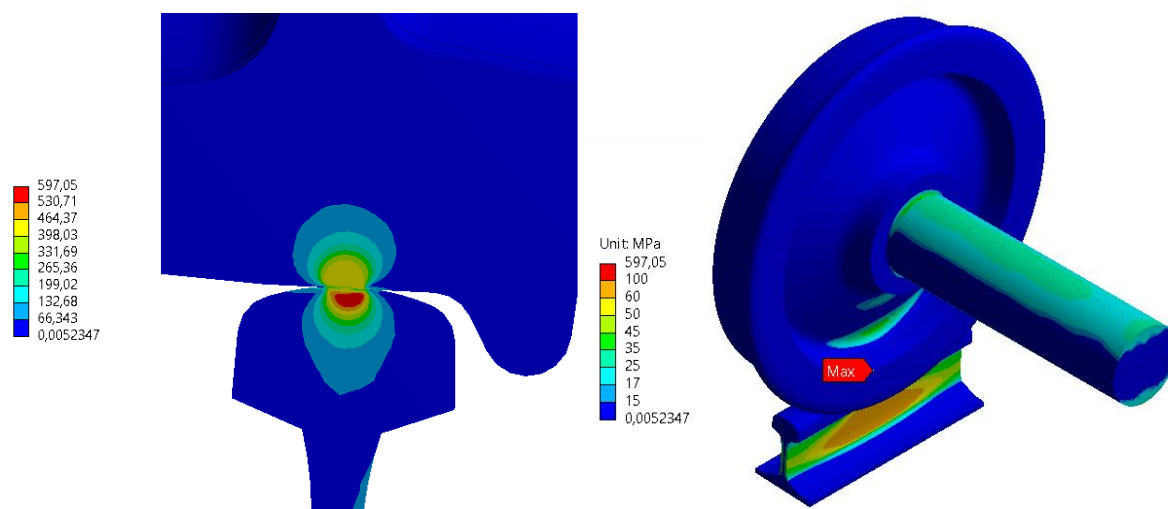


Figure 7. Von Mises stress [MPa] distribution on global model for $\mu = 0.25$.

Equivalent plastic strains results shown in Figure 11, reveal that most of the plastic deformation occurs at the wheel, on the contrary almost very small plastic deformation occurs at the rail. Although maximum strain for the wheel is calculated 4% at a node, similar value for neighboring nodes found to be 1,2% and 1,3%, thus implying high strain gradient on a single element on the neighboring mesh layers that could be attributed to stress concentration where the maximum equivalent plastic stress occurs right on the same node around 462 MPa as also shown in Figure 12.

If we look at the wheel and rail von-Mises stress contours more closely as presented in Fig. 8,9, we visualize the crack which is occurring during the operating cycle, exactly in the area where shown in Fig. 8,9.

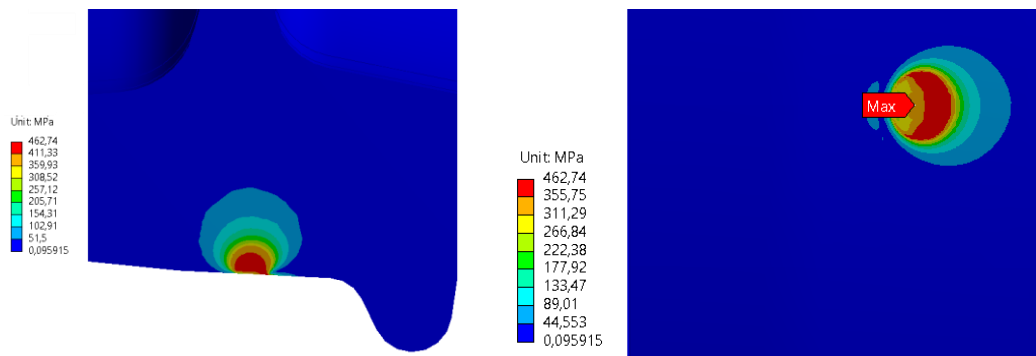


Figure 8. Von Mises stress [MPa] distribution on wheel for $\mu = 0.25$.

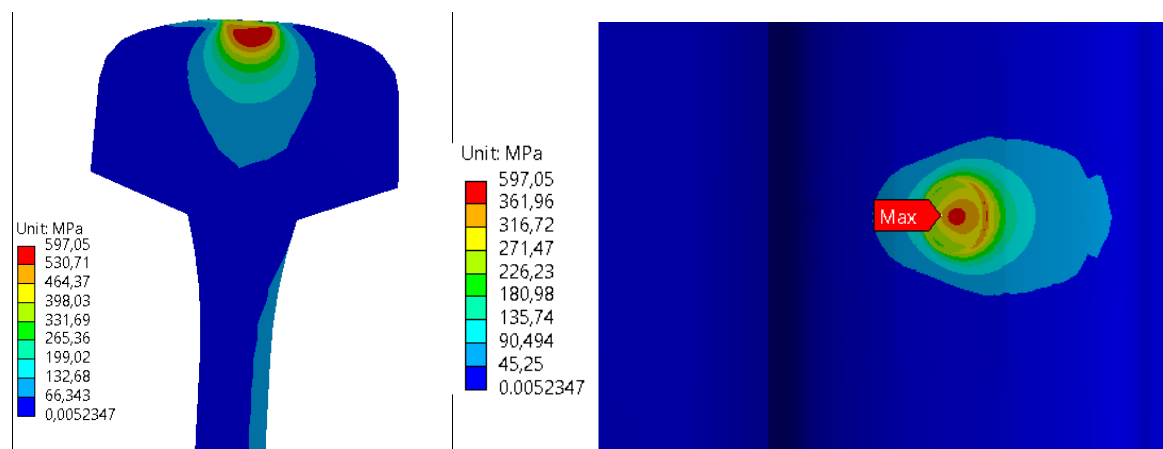


Figure 9. Von Mises stress [MPa] distribution on rail for $\mu = 0.25$.

In Fig. 10 - 12, Von Mises elastic strain found around 3%, clearly depicting high strain level. Von Mises plastic strain in Figure 13 also shows very low plastic deformation occurring on the surface of the wheel but towards 3,32 mm interior of the surface some strain peak is observed due to edge effect and low mesh density in this area.

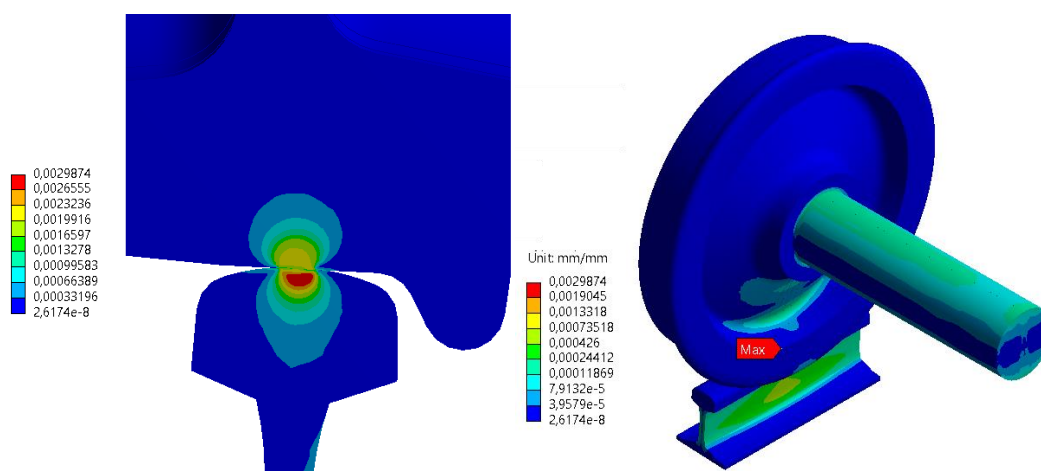


Figure 10. Von Mises elastic strain [mm/mm] distribution on global model for $\mu = 0.25$.

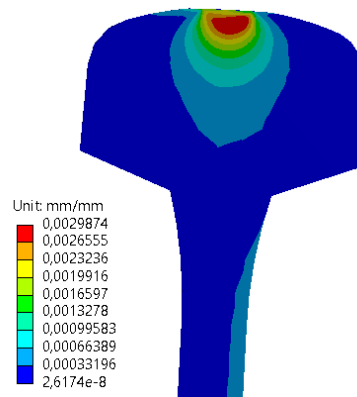


Figure 11. Von Mises elastic strain [mm/mm] distribution on rail for $\mu = 0.25$.

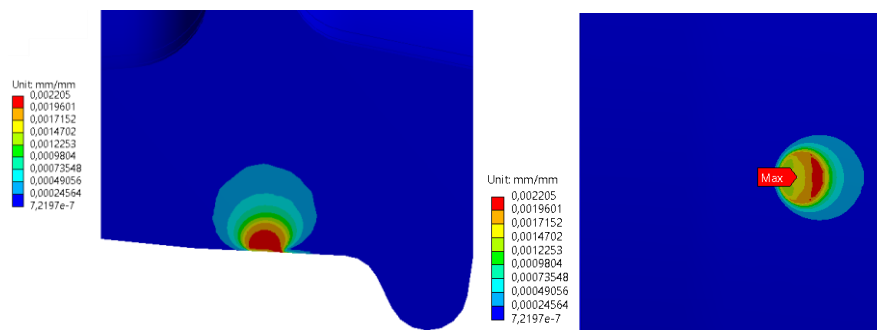


Figure 12. Von Mises elastic strain [mm/mm] distribution on wheel for $\mu = 0.25$.

Figure 8 shows maximum equivalent stress of about 462 MPa found on the surface of the wheel over the yield stress with stress contours shown.

Von Mises elastic strain of about 2,2% found on the surface of the wheel with a maximum value again on the surface with a spot of 1,9% as shown in Fig. 10, railway wheel flat occurring due to elastic deformation during contact is also very visible. On the contrary, there is almost no plastic deformation observed on the surface of the wheel, except at very tiny two symmetric dot shaped locations. Finally, contact status, penetration and pressure levels are also presented in Figure 15-19. Contact status exhibits almost elliptical shape of the contact sticking similar to contact penetration parameter contour and maximum contact Pressure obtained around 960 MPa in the center of the ellipse.

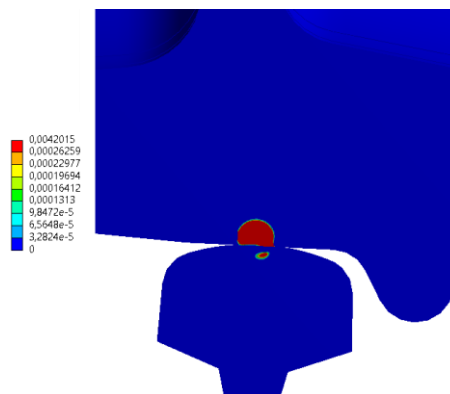


Figure 13. Von Mises plastic strain [mm/mm] distribution on global model for $\mu = 0.25$.

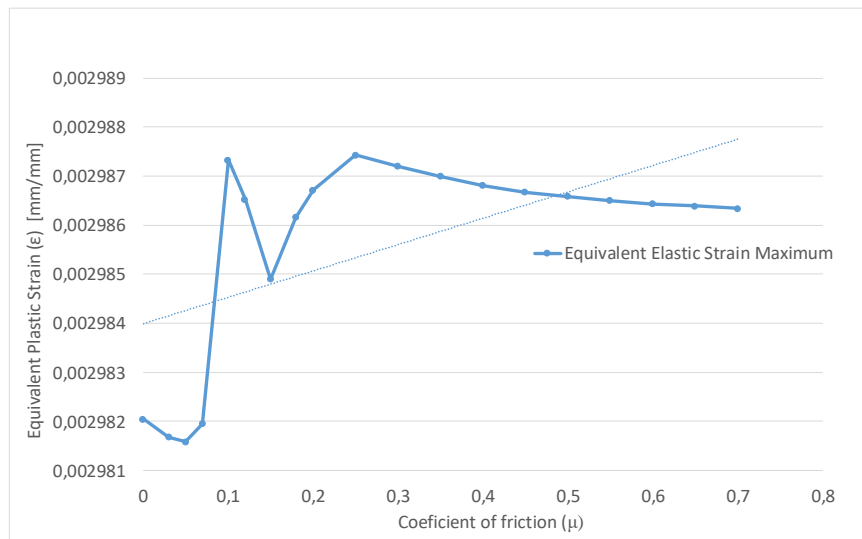


Figure 14. Maximum von Mises elastic strain [mm/mm] distribution on global model for all scenarios.

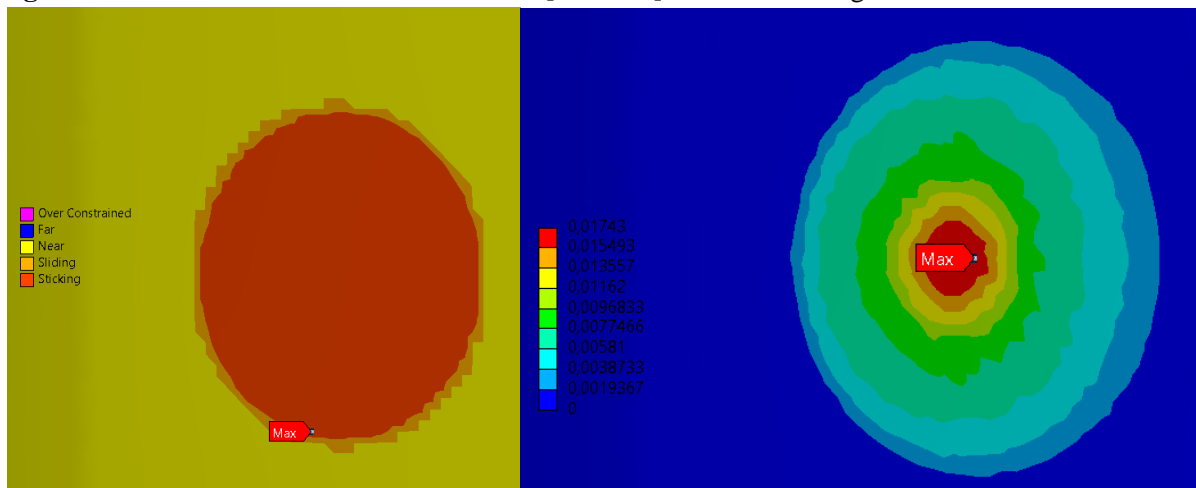


Figure 15. Contact status and sliding distance [mm] for $\mu = 0.25$.

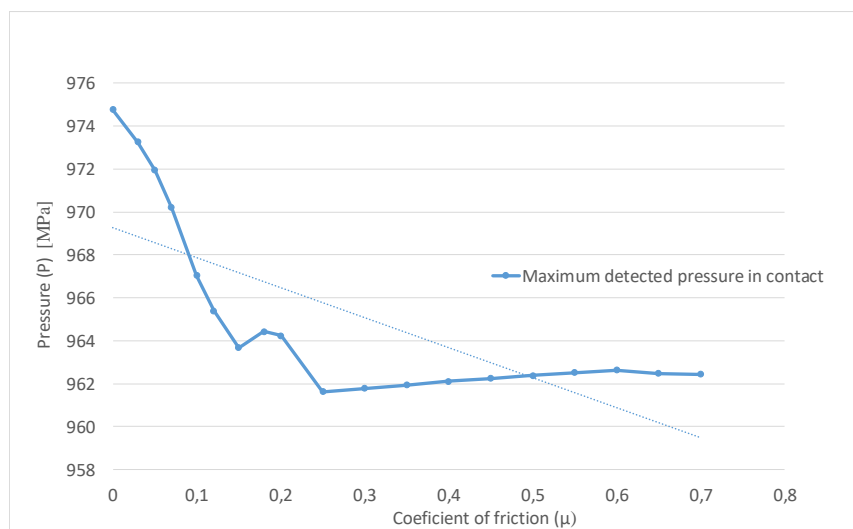


Figure 16. Pressure [MPa] gradient for all FEA scenarios.

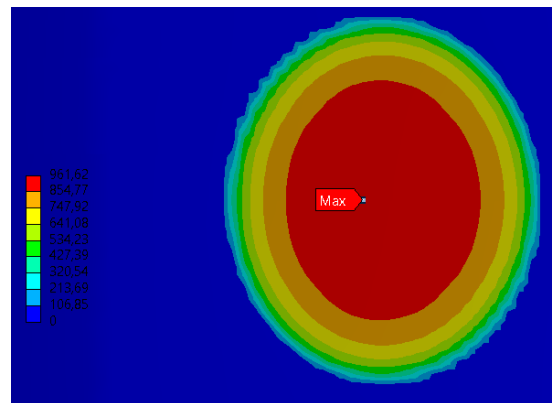


Figure 17. Pressure [MPa] gradient for $\mu = 0.25$.

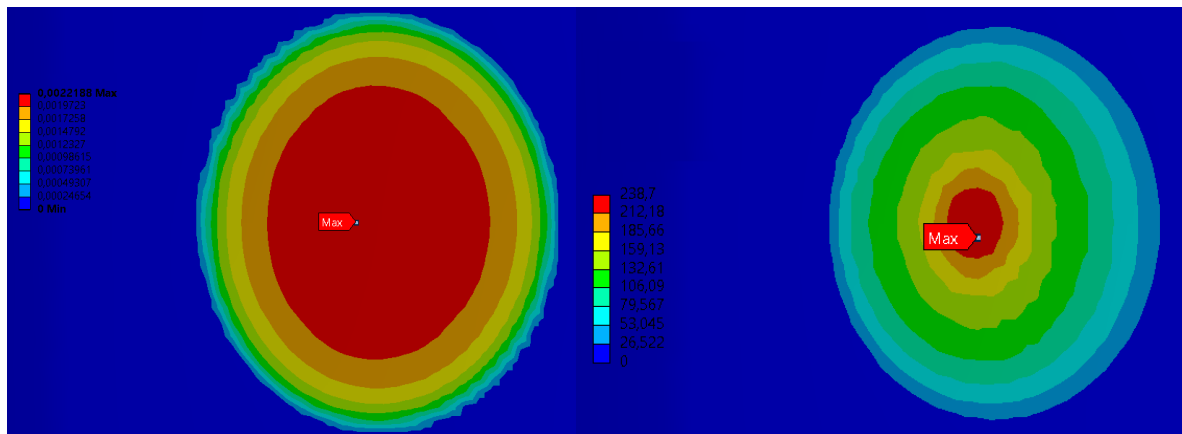


Figure 18. Penetration [mm] and frictional stress [MPa] for $\mu = 0.25$ scenario.

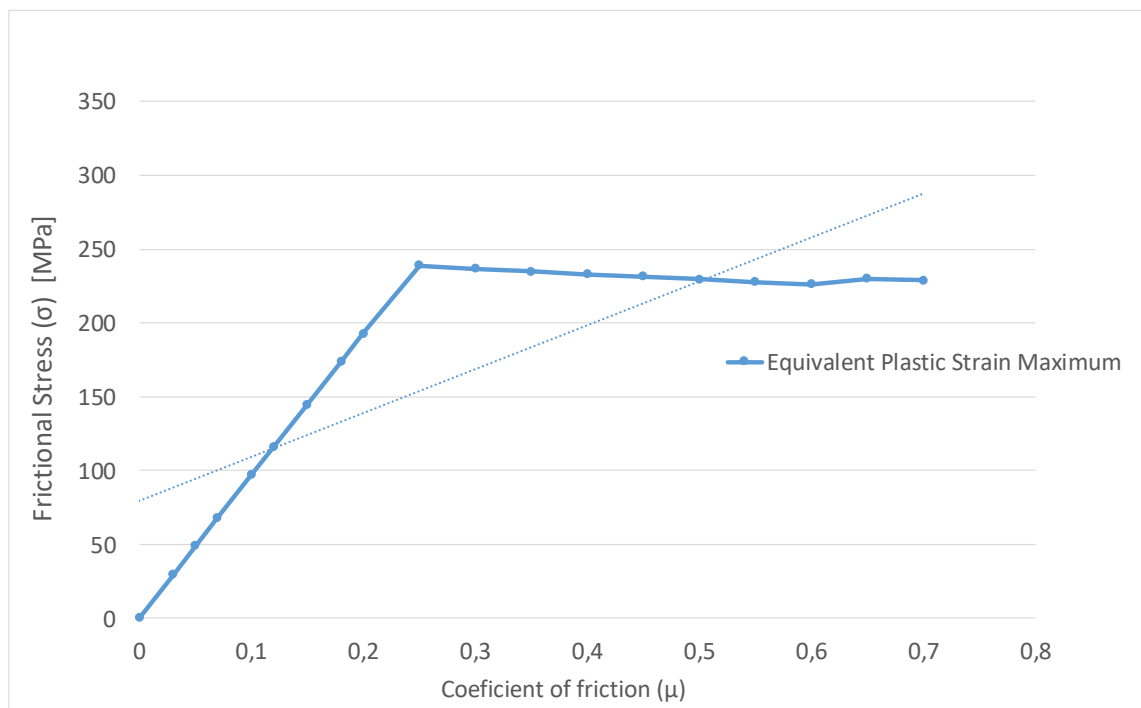


Figure 19. Frictional stress [MPa] for all FEA scenarios.

4. Conclusions

In this work has been achieved, pressure distribution according to the elastic pattern, for interaction between a wheel with profile S78 and a rail UIC 60, with the tilt 1/20 and friction coefficient in wheel – rail contact get values between 0 – 0,8, the Von Mises equivalent stress state at the wheel-rail contact, according to the model elastic – plastic.

The presence of friction forces on the contact field causes the effects:

- a) asymmetric distribution of Von Mises stress;
- b) increasing the maximum stress value Von Mises and locating the maximum value at smaller y-depths.

Both the increase in the relative value of the Von Mises equivalent stress, as well as the proximity of the maximum point contact surface influences negatively the durability of the wheel and rail fatigue, which works under a rolling contact request.

References

- [1] Crețu S 2009 *Contactul concentrat elastic-plastic*” (Editura „Politehniun”, Iași)
- [2] Vo K D, Tieu A K, Zhu H T and Kosasih P B 2014 A tool to estimate the wheel/rail contact and temperature rising under dry, wet and oily conditions *COMPRAIL 14th Conference on Railway Engineering Design and Optimization* United Kingdom: WIT Press pp. 191-201
- [3] Zhang J, Shouguang S and Xuesong J 2009 *Numerical simulation of two-point contact between wheel and rail* (AMSS Press, Wuhan, China)
- [4] Cui X L, Chen G X, Yang H G, Zhang Q, Ouyang H and Zhu M H 2015 *Effect of the wheel/rail contact angle and the direction of the saturated creep force on rail corrugation* (Elsevier B. V.)
- [5] Xin Z, Xiaogang Z, Chao L, Zefeng W and Xuesong Jin 2016 *A study on dynamic stress intensity factors of rail cracks at high speeds by a 3D explicit finite element model of rolling contact* (Elsevier B. V.)
- [6] Wang W J, Lewis R, Yang B, Guo L C, Liu Q Y, and Zhu M H 2016 *Wear and damage transitions of wheel and rail materials under various contact conditions* (Elsevier B. V.)
- [7] Peixoto D F C et al. 2007 *Non-linear analysis of the wheel/rail contact* (Departamento de Engenharia Mecânica, Faculdade de Engenharia da Universidade do Porto Portugal)
- [8] Busquet M et al. 2003 3D Finite element investigation on the plastic flows of railheads. *Correlation with micro structural observations. In: 6th International conference on contact mechanics and wear of rail/wheel systems CM2003* in Gothenburg, Sweden.
- [9] Zili L, Xin Z, Coenraad E, Rolf D and Molodova M 2008 *An investigation into the causes of squats—Correlation analysis and numerical modelling* (Elsevier B.V.)
- [10] Wen-jian W, Wen-juan J, Heng-yu W, Qi-yue L, Min-hao Z and Xue-song J 2016. *Experimental study on the wear and damage behavior of different wheel/rail materials* (Journal of rail and rapid transit)
- [11] Romanian standard STAS 112/3-90 *Aparate de rulare pentru vehicule de cale ferată cu ecartament normal. Bandaje în stare prelucrată pentru roți. Dimensiuni*
- [12] Romanian standard SR EN 13674 *Aplicații feroviare. Cale. Șine*